ACS central science

Research Article

http://pubs.acs.org/journal/acscii

Crowding and Anomalous Capacitance at an Electrode−Ionic Liquid Interface Observed Using Operando X-ray Scattering

Miaoqi Chu, Mitchell Miller, and Pulak Dutta*

Department of Physics & Astronomy, Northwestern University, Evanston, Illinois 60208, United States

Supporting Information

ABSTRACT: Room temperature ionic liquids are widely recognized as novel electrolytes with properties very different from those of aqueous solutions, and thus with many potential applications, but observing how they actually behave at electrolytic interfaces has proved to be challenging. We have studied the voltage-dependent structure of $[TDTHP]^+[NTF_2]^-$ near its interface with an electrode, using in situ synchrotron X-ray reflectivity. An anion-rich layer develops at the interface above a threshold voltage of +1.75 V, and the layer thickness increases rapidly with voltage, reaching ∼6 nm (much larger that the anion dimensions) at +2.64 V. These results provide direct confirmation of the theoretical prediction of "crowding" of ions near the interface. The interfacial layer is not purely anionic but a mixture of up to ∼80% anions and the rest cations. The static differential capacitance calculated from X-ray measurements shows an increase at higher voltages, consistent with a recent zero-frequency capacitance measurement but inconsistent with ac capacitance measurements.

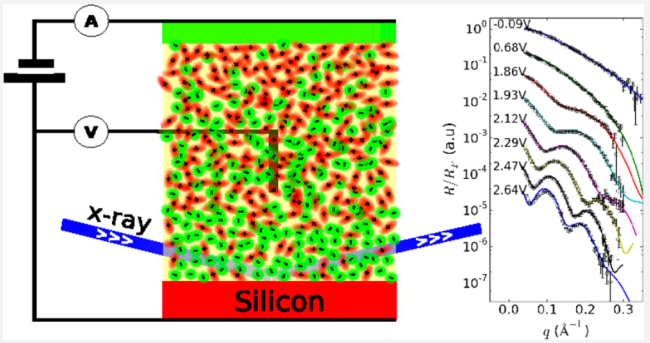

INTRODUCTION

Room temperature ionic liquids (RTILs) are salts with molecular anions and/or molecular cations, which are in the liquid phase at or near room temperature.[1,2] They are typically nonvolatile, do not require the presence of solvents to be liquid, and have large electrochemical windows. Over the past decade there has been an explosion of interest in ionic liquids, driven both by the synthesis of many different anions and cations[3] and by potential applications that range from electrolytes to supercapacitors to electrically controlled lubricants to electrodeposition of metals and alloys.[4−6]

Central to the presumed novelty of RTILs is the idea that the molecules are largely dissociated, i.e., the liquids have very high ionic densities (although this has been disputed[7−10]). Further, the molecular ions are much larger than typical ions in aqueous solutions, and often have irregular shapes. Thus, there is general agreement that RTILs must behave very differently from aqueous solutions, in particular at interfaces. For example, the Gouy−Chapman−Stern (GCS) picture of the electrolyte near an electrode[11] predicts a tightly bound Stern monolayer followed by a diffuse monotonic charge distribution. This picture has been found to be applicable at a variety of dilute electrolytes near electrodes,[11] and has been directly confirmed by X-ray standing wave studies.[12] However, the differential capacitance of the RTIL−electrode interface shows anomalous behavior as a function of voltage, frequency, etc.: the curves are bell-shaped or camel-shaped, which are inconsistent with the GCS picture.[5,7,13] This behavior must originate from the nanoscale structure of RTILs near electrode interfaces, but what that structure is and how it depends on the applied voltage are poorly understood.

As is frequently the case with liquids, a considerable amount of information about interfacial RTILs comes from the predictions of simulations and mean field theories rather than from (relatively difficult) experiments. For example, Kirchner et al.,[14] using molecular dynamics, predict a multilayer structure (alternating anions and cations) at low surface charge, with a transition to a dense counterion monolayer as the electrode surface charge increases. Kornyshev[13] predicted crowding (formation of a thick counterion layer) using mean field theory. A progression from overscreening (with alternating anion/cation layers) to crowding as a function of ion density, charge, or voltage has been observed in molecular dynamics simulations[7,15,16] and Landau−Ginsburg theory.[17−19] Ivaništšev et al.,[20,21] using molecular dynamics, also predict the formation of an alternating cation−anion layered structure that transitions to a crowded interface layer at higher surface charge. These predicted structures, which are different from those expected in aqueous solutions of ions, may help explain why systems using RTIL electrolytes behave differently from traditional electrolytes. (It is impractical to provide a comprehensive review of the status of the theory here; see ref 22 for an overview.)

There are only a few experimental tools that can look at the nanoscale charge distribution normal to an RTIL−solid interface. X-ray and neutron reflectivity are two such tools.

Received: January 18, 2016
Published: March 7, 2016

DOI: 10.1021/acscentsci.6b00014
ACS Cent. Sci. 2016, 2, 175−180

Neutrons have been used to study RTILs,[23,24] and have significant advantages in studies of organic molecules that can be selectively deuterated. However, synchrotron X-ray beams have much higher usable flux for studies requiring a low incidence angle at a surface or interface. X-rays are only sensitive to the total electron density and cannot distinguish anions from cations based on their charge. However, the anion and cation will in general have different electron densities, and thus a nonuniform electron density profile at an electrode−RTIL interface means that there is a nonuniform interfacial charge density profile.

There have been several previous studies of RTIL structure near solid surfaces[25−28] where there is no applied voltage and no way to measure the surface charge in situ. In refs 25 and 26, the reflectivity data for an RTIL on insulating (sapphire) substrates, assumed to be charged due to X-ray exposure, were fitted assuming alternating cation/anion layers. However, in ref 27 similar layering was reported using uncharged (hydroxylated) sapphire. Thus, Uysal et al.[29] have correctly noted that the observed layering may have the same origin as that seen even in nonionic molecular liquids.[30] Reference 28 reported a dense layer at a presumably uncharged graphene surface, but alternating cation and anion layers at a presumably charged mica surface.

There have also been some X-ray studies of RTIL structure using applied voltages at conducting substrates (electrodes). Yamamoto et al.[31] used a gold electrode and determined the X-ray reflectivity at one positive and one negative voltage; these differed slightly. Although the reflectivities were monotonic (no interference maxima or minima), the data were fitted using a distorted crystal model (implying layering at the interface). Uysal et al.[32] used epitaxial graphene on SiC wafers as the electrode, and also reported alternating anion/cation layers in the interfacial RTIL studied at the largest positive and negative voltages used. In a subsequent work, Uysal et al.[29] studied the same RTIL at intermediate voltages, and found that the structure was a combination of the two extreme-voltage structures.

Experiments using force measurements, the only other applicable technique with comparable spatial resolution normal to the interface, also reach a variety of conclusions. Atomic force microscopy data indicate layered structures near gold[33] and pyrolytic graphite[34] electrodes, with the number of layers being a function of applied voltage. However, measurements using a surface force apparatus,[9] which can be thought of as replacing the AFM tip with an essentially flat mica surface, indicate the presence of an adsorbed ion layer followed by a monotonic diffuse distribution, consistent with the GCS model.

Our X-ray reflectivity study departs from previous studies in crucial ways. First, since gold has an extremely high electron density (4660 electrons/nm^3, over an order of magnitude greater than typical ionic liquids), the X-ray reflection from gold[31] swamps the reflection from RTIL interfacial structures of interest. We used H-terminated silicon substrates instead: silicon has an electron density of ∼700 electrons/nm^3, only about twice that of the typical RTIL. In the Supporting Information we show that a given interfacial structure will lead to visible interference features in the X-ray reflectivity if the substrate is silicon, but not if it is gold. Second, we used an RTIL that has a wide electrochemical window, allowing us to apply higher voltages, as well as a strong electron density contrast between anion and cation. We performed a detailed study as a function of voltage, rather than one or two voltages as in some previous studies.[31,32] This allowed us to observe clear trends in the interfacial structure as a function of the applied voltage. Our results differ substantially from those reported in ref 29, but note that the RTILs studied were not exactly the same (same anion, different cation).

It should be noted that the use of a semiconductor electrode introduces some complexities[11] when the electrolyte is a better conductor than the electrode. That is not the case here: the RTIL electrical conductivity (∼1−10 mS/cm) is much lower than that of the p-type silicon substrates we used (33−1000 mS/cm). Further, all our observations were performed within the electrochemical window and thus at negligible current density.

RESULTS AND DISCUSSION

The RTIL studied was trihexyltetradecylphosphonium bis-(trifluoromethylsulfonyl)imide ([TDTHP]$^+$[NTF$_2$]$^-$), see Figure 1. See Methods for a description of our experimental layout.

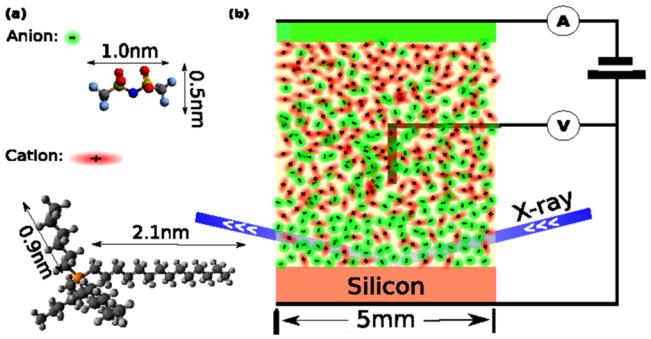

Figure 1. (a) The dimensions and molecular structures of anion and cation used in our experiment. Atoms are represented by colors as follows: red = O, dark blue = N, yellow = F, light blue = S, orange = P, black = C, gray = H. Black and gray spheres are C and H atoms. (b) Schematic diagram of the experiment, showing the grazing incidence X-ray geometry (angle of incidence exaggerated).

Figure 2 shows a cyclic voltammogram obtained using our experimental setup. The electrochemical window (EW), within which it is assumed that there is no electrolysis, is typically defined as the voltage range in which the current is less than 0.1−1.0 mA/cm^2.[35] The ions in our RTIL, [TDTHP]$^+$ and

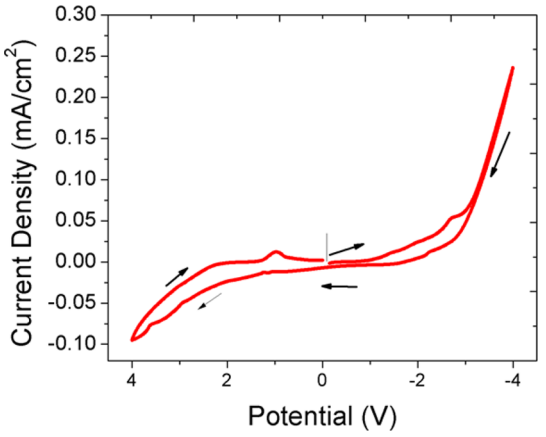

Figure 2. Cyclic voltammogram for [TDTHP]$^+$[NTF$_2$]$^-$ measured in our experimental setup, i.e., with Si and Au electrodes.The vertical line and arrows indicate the starting point and scan direction.

DOI: 10.1021/acscentsci.6b00014
ACS Cent. Sci. 2016, 2, 175−180

$[NTF_2]^-$, have some of the largest electrochemical-window potentials among common RTIL anions and cations,[5,35,36] −3.64 V and +2.70 V respectively. Figure 2 is consistent with these numbers.

X-ray reflectivity data depend on the electron density profile normal to the reflecting interface, $\rho_s(z)$, averaged over the interface plane (i.e., over the x- and y-directions). As previously noted, X-rays are sensitive to the total electron density, including all electrons in each atom. In the RTIL studied, there is a significant difference between the sizes and electron densities of the anion and cation. The bulk RTIL has electron density ρ_{IL} = 347 electrons/nm^3. The cation is large (0.95 nm^3) and has only slightly lower density than the bulk liquid (289 electrons/nm^3), while the anion is small (0.24 nm^3) and is much denser than the bulk (577 electrons/nm^3). (See the Supporting Information for the origin of these numbers.) The difference in electron density allows us to interpret any deviations from the bulk RTIL electron density as due to an imbalance between cations and anions, and thus to calculate the charge density. Specifically, assuming that the cation (anion) carries charge of Q ($-Q$), the charge density ρ_c can be calculated from

$$\rho_c = Q(\rho_s - \rho_{IL})\frac{V_a + V_c}{V_a N_c - V_c N_a} \quad (1)$$

where ρ_s and ρ_{IL} are the electron density at the interface and the average electron density of the bulk ionic liquid. V_a (V_c) and N_a (N_c) are the effective volume of, and number of electrons in, one anion (cation). Note that this equation does not allow for compression at the interface (which would change V_a and/or V_c), and assumes that the ions do not have fractional charge. These possibilities are discussed later in the paper.

The etched silicon (111) surface can undergo surface reconstruction,[37] leading to a relatively rough surface which causes interfacial reflectivity data to drop rapidly with increasing q. Flux attenuation during transmission through the bulk RTIL, and scattering background from bulk IL (which has a broad peak around 0.41 Å^{-1}), further reduce the highest momentum transfer in a reflectivity scan q_{max} to 0.30 Å^{-1}, corresponding to a spatial resolution function of width π/qmax ≈ 1 nm.

Figure 3 shows X-ray reflectivity data R divided by the ideal Fresnel reflectivity R_F, as a function of applied voltage (measured between the Si substrate and the reference electrode). At negative voltages (Si electrode at negative potential relative to the reference electrode), the reflectivity curves are featureless. We attribute this to the poor density contrast between the bulk liquid and the cations that are presumably attracted to the electrode surface. These data are not shown in this paper. For positive voltages, the reflectivity curves are featureless at low voltages. Featureless curves can still be (and often are) fitted with postulated models, but the conclusions are not robust. However, at higher voltages, oscillations begin to appear, and the minima shift to lower q as the applied voltage increases. Such oscillatory features allow more definitive fits to the data. At each voltage, it takes about 20 min for the reflectivity curve to become stable, i.e., for the interfacial structure to form. The data are then stable over a period of at least 40 min, showing that they are not electrolysis products collecting with time. Our data were also reproducible in multiple samples.

The general procedures for fitting X-ray reflectivity data have been discussed elsewhere. Here we address the choice of model

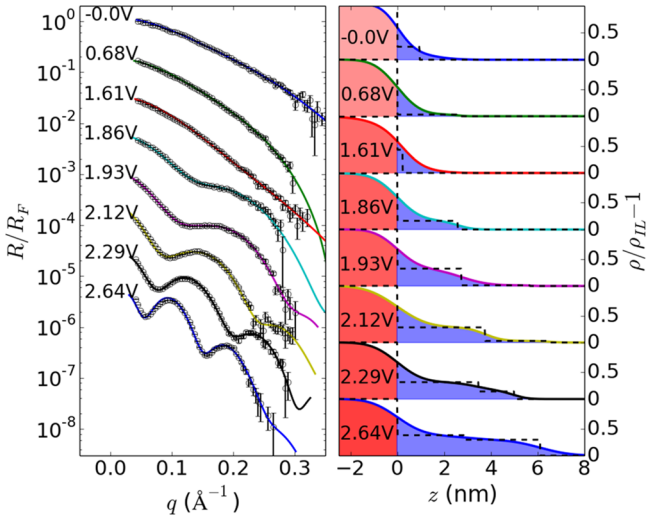

Figure 3. Left: voltage dependent X-ray reflectivity data (open circles) and fits using the slab model discussed in the text (solid lines). The curves are shifted vertically relative to each other for clarity. Right: the voltage-dependent electron density enhancement profiles, $(\rho(z) - \rho_{IL})/\rho_{IL}$ where ρ_{IL} is the bulk liquid density, obtained from slab model fits to the data. The dashed lines show the slabs without interface broadening (roughness); the smooth curves show the roughness-broadened profiles. red = Si electrode; blue = anions.

to fit the data. In many previous studies,[25,31,38] a distorted crystal model has been used to fit the reflectivity curve. In this model as applied to an ionic liquid, there are alternating layers of cations and anions, with each layer having the same charge but becoming increasingly diffuse (broad) until the structure becomes that of the bulk liquid. This might happen if there is overcharging: the first layer of anions carries more charge than necessary, which requires a subsequent layer of anions, resulting in charge oscillations decaying into the bulk liquid. When there are maxima and minima in the reflectivity, a simple slab model (interfacial steps of variable width, density, and interface roughness) will also fit the data.

We have found that the distorted crystal model will fit our data only if the Si surface is given a very large roughness (>2 nm), and this indicates that there is a dense interfacial layer that the distorted crystal model by itself cannot capture (see Supporting Information for details). The authors of ref 32 have also found that the distorted crystal model must be supplemented with an interfacial slab to fit the data from a similar system. Further, since our data were collected at multiple voltages and show the reflectivity minimum moving to smaller q with increasing voltage, the thickness of every layer in the alternating-layer picture would have to increase continuously with voltage, which is not expected in the distorted crystal model. We are able to fit our data with interfacial slabs, without adding alternating anion−cation layers. Of course, a slab model is also an approximation to reality: it is a "pixelated" representation of the actual density profile, taking into account the finite spatial resolution of the reflectivity technique.

As shown in Figure 3, the reflectivity curve is featureless at and below 1.61 V, but develops features (fringes) above that voltage. We fitted all data using either one or two slabs, but when there are no features, the fits naturally do not give significant results. Up to 2.12 V, the data can be fitted using just one interfacial slab. The data at higher voltages can also be fitted with one slab, but the fit is slightly improved by using two

DOI: 10.1021/acscentsci.6b00014
ACS Cent. Sci. 2016, 2, 175−180

adjacent slabs. This suggests that the actual electron density profile is rounded such that two "pixels" represent the actual profile better than one uniform-density slab can. However, the basic features of the interfacial region (total thickness, average density) remain essentially the same whether a one-slab or two-slab fit is used.

The fitting parameters are tabulated in the Supporting Information. Figure 4 shows the slab thickness (total thickness

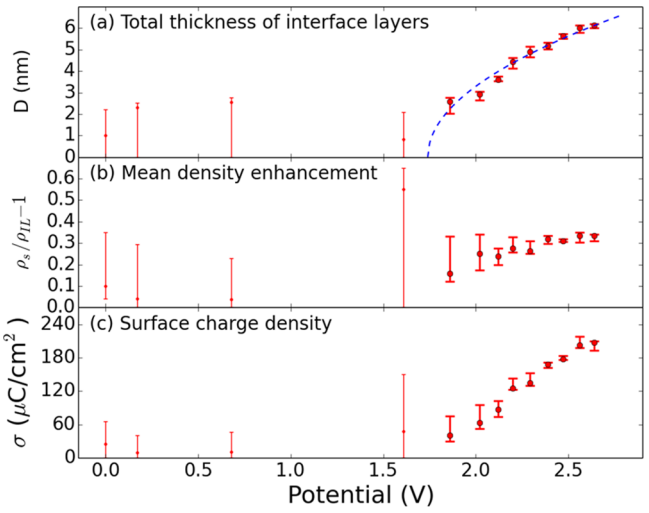

Figure 4. Best-fit parameters as a function of voltage. (a) Slab width (for one-slab fits) or total width of interface slabs (for two-slab fits). The dashed line is a fit to $D \propto \sqrt{(V - V_{th})}$ where V_{th} is a threshold voltage. (b) The interfacial slab electron density enhancement $(\rho_s - \rho_{IL})/\rho_{IL}$ where ρ_{IL} is the bulk liquid electron density (mean enhancement is shown for two-slab fits). (c) Surface charge density (anionic charge per unit area), calculated from the slab electron density assuming that the effective volumes of the cations and anions, and their charges, are fixed (these assumptions are discussed in the text).

if two slabs), electron density enhancement (average enhancement if two slabs), and calculated surface charge density as functions of voltage. The qualitative trends are as follows. For lower voltages, when the reflectivity has no oscillatory features, the error bars are large and include zero. At higher voltages the interfacial density is higher than the bulk density, and this means that there is an excess of anions over cations, as one would expect. The average electron density varies only weakly with voltage, and never reaches the density of the anion. At most the interfacial layer averages ~80% anions, ~20% cations (this is the number ratio; in terms of volume it is ~60% anions, ~40% cations). This layer is not a monolayer; rather, above a threshold voltage $V_{th} \approx 1.75$ V the slab thickness D increases rapidly with voltage until it is ~6 nm, much larger than the anion dimensions.

These data are consistent with the formation of a crowded layer at higher voltages, as predicted[7,13,15−18,21] but never before observed, with the thickness being a strong function of the applied voltage. Since the lower-voltage data show no fringes, there is no significant evidence in our data of any interfacial structure below the threshold voltage. Nonetheless, the existence of this threshold voltage requires explanation. It is likely that, for $V < V_{th}$, the interfacial electric field is balanced out either by weak alternating layers of cations and anions or by a diffuse Gouy−Chapman double layer as in ionic solutions. However, these structures would have to be too weak to have any signature in our X-ray reflectivity data.

If there is a potential difference $V - V_{th}$ across a uniform charged slab of thickness D, Gauss's law applied to a charged slab requires that $D^2 = (\varepsilon_o\varepsilon_r/\rho_c)(V - V_{th})$ where ρ_c is the charge per unit volume and ε_r is the relative permittivity of the material. (This equation, except for the threshold voltage V_{th}, is equivalent to eq 23 of ref 13.) Figure 4b shows that the electron density of the slab is at most weakly V-dependent; if we ignore this weak dependence and assume that the slab electron density ρ_s and therefore the charge density ρ_c do not depend on V, we get $D = \lambda\sqrt{(V - V_{th})}$ where $\lambda \equiv \sqrt{(\varepsilon_o\varepsilon_r/\rho_c)}$ is a constant. The dashed line in Figure 4a shows the best fit to this functional form. Clearly the data are consistent with the predicted V dependence. This fit gives us $V_{th} = 1.75$ V and $\lambda = 6.45$ nm $V^{-0.5}$.

The data in Figure 4c, which give the interfacial charge per unit area, allow us to estimate the static (zero-frequency) differential capacitance. Because of the scatter in the $\sigma-V$ data, it is not possible to plot the derivative $d\sigma/dV$ as a function of V in any detail. However, we can say that, below V_{th}, the differential capacitance due to the dense layer is indistinguishable from zero in our experiments, while at higher voltages the average slope gives us ~200 μF/cm^2. (These numbers are in addition to the capacitance due to any effects not observed in our X-ray studies.)

The calculated capacitance above V_{th} is high compared to numbers typically reported for RTILs using ac measurements (~10−20 μF/cm^2). On the other hand, it is known[39] that RTIL interfacial capacitance depends on frequency as $\omega^{-\alpha}$ where $\alpha \approx 0.1-0.3$, which (if rigorously true) would diverge in the dc limit. This suggests that the dc capacitance of electrode−RTIL interfaces is larger than that seen using ac measurements. The source of such a difference would be the known low mobility of RTIL ions. Indeed, a recent dc capacitance measurement[40] on a different RTIL found that the differential capacitance increases at the highest voltages studied, and reaches >50 μF/cm^2. This increase is inconsistent with the "camel-shaped" or "bell-shaped" curves found in ac measurements, but qualitatively consistent with what we observe.

A second anomaly concerns the factor λ. From the electron density data in Figure 4b: we find that the charge density ρ_c is approximately 3×10^{-19} C/nm^3 at 2.64 V. Using this value and the typical range of ε_r for bulk RTILs (~15−20),[5] we estimate that $\lambda \sim 0.6$ nm $V^{-0.5}$. This is an order of magnitude smaller than the value obtained by fitting the $D-V$ curve, and may imply that the actual charge density is lower, the relative permittivity is higher, or both.

Two factors not yet considered may reduce our estimates of the surface charge density (Figure 4c). First, in the bulk RTIL, it has been suggested that the actual ionic charges are not integers but ~0.6−0.8 electrons/ion.[41−44] Second, in common with previous X-ray studies,[25−32] our calculations above interpreted electron density changes as due purely to anion/cation imbalance, without considering the possibility of compression or expansion at the interface. Lattice gas models of RTILs[13] assume large fractions of unoccupied sites, using a parameter γ defined as the ratio of actual to maximum ionic concentration (so that $1 - \gamma$ is the free volume fraction), and suggest that γ may be as low as 0.5 even in pure RTILs. Experimentally, however, RTILs do not appear to be very compressible. Reference 45, using a different RTIL, reports only a ~5% increase in density at 120 MPa (~1200 atm)

DOI: 10.1021/acscentsci.6b00014
ACS Cent. Sci. 2016, 2, 175−180

pressure. Figure 4b shows that our interfacial density increases by up to 25−30% above the bulk density. It is physically unreasonable to attribute any voltage-dependent density change to compression alone, without attracting anions to the interface, since there would then be no driving force for such compression. Nonetheless our experiments cannot rule out an unspecified combination of compression, fractional charges per ion, and anion crowding. This would quantitatively reduce but not qualitatively eliminate the charge present in the dense layer (Figure 4c), and thus it would reduce the estimated capacitance. Our measurements of the voltage-dependent thickness of the crowded layer (Figure 4a) and our qualitative conclusion that the capacitance increases across the threshold voltage are, however, robust.

We have performed the same experiments with two other RTILs (data not shown here). $[TDTHP]^+[Cl]^-$, which has the same cation but a different anion, gave a null result, while $[N4111]^+[NTF_2]^-$, which has the same anion but a different cation, showed qualitatively similar behavior to that reported above. This is reasonable: a Cl^- anion carries only 17 electrons while $[NTF_2]^-$ carries 138 electrons, so that for the same amount of interfacial change, the chloride anion would create a much smaller interfacial electron density enhancement. This also shows that the interfacial layer must be attributed to the dense $[NTF_2]^-$ anion, and not to spurious effects such as electrolysis products.

Our results provide direct confirmation of the theoretical prediction that there will be a thick "crowded" layer of ions near an electrode interface at higher voltages. This layer develops only above a threshold voltage V_{th}. Unexpectedly, the crowded layer is not purely anionic, but at most ∼80% anions and 20% cations. We see no evidence of either alternating layers of anions and cations ("overcharging") or a diffuse layer in our system, although it is likely that there are interfacial structures below our level of detection. Further, our data imply that the dc differential capacitance is larger at higher voltages, and the permittivity of the interfacial layer may also be large. Both these possibilities have significant implications for the use of RTILs for energy storage and in electrochemical devices, and illustrate the complexity and novelty of this class of liquid electrolytes.

METHODS

Trihexyltetradecylphosphonium bis(trifluoromethylsulfonyl)-imide ($[TDTHP]^+[NTF_2]^-$) was purchased from Stem Chemicals. Figure 1 shows the anion and cation. The RTIL was placed in a vacuum oven for 24 h to remove water at 373 K. P-type (111) silicon chips (5 mm × 7 mm) were purchased from Ted-Pella. To obtain an atomistic flat surface,[46] we used a rapid thermal process (AW-610) in oxygen to grow a layer of thermal oxide of ∼400 Å on the silicon surfaces. This layer was removed with buffered oxide etch, exposing ultraflat fresh silicon (111) surfaces. The silicon chip was mounted to a transmission cell (made of Kel-F, with Kapton windows) and connected as the working electrode. Gold wires were used to electrically connect to the chip, and also used as counter and pseudoreference electrodes within the liquid. Although a thin liquid film sample cell[31,47] causes less attenuation of X-rays traveling through the RTIL, we did not use such a setup because of the high resistivity of RTILs and the resulting risk of nonuniform interfacial potential. The external voltage was controlled with a potentiostat (DY2311, Ivy-Digital).

Figure 1 shows the layout of the experiment. The specular reflectivity was measured in the transmission geometry as a function of wave transfer, $k = 2\pi \sin \theta/\lambda$. The thickness of the transmission cell in the direction of the X-ray beam was 6 mm, and the width of the silicon substrate in the beam direction was 5 mm. The experiment was conducted at Sectors 12BM-B and 33BM-C of the Advanced Photon Source, with X-ray energy of 19.3 keV. An area detector Pilatus 100 K was used to simultaneously record the specular reflectivity signal as well as the off-specular background (±0.2 degree off the specular beam in the χ direction).

ASSOCIATED CONTENT

Supporting Information

The Supporting Information is available free of charge on the ACS Publications website at DOI: 10.1021/acscentsci.6b00014.

Best-fit parameters, comparison of one- and two-slab model fits, electron density data, rationale for choice of Si electrode, and results of attempted fitting using the distorted crystal model (PDF)

AUTHOR INFORMATION

Corresponding Author

*E-mail: pdutta@northwestern.edu.

Notes

The authors declare no competing financial interest.

ACKNOWLEDGMENTS

This research was supported by the U.S. National Science Foundation under Grant No. DMR-1309589. This work utilized Northwestern University's Micro/Nano Fabrication Facility (NUFAB), which is supported by the State of Illinois and Northwestern University. The X-ray reflectivity measurements were performed at Beamlines 12BM-B and 33BM-C of the Advanced Photon Source, which are supported by the U.S. Department of Energy under Contract No. DE-AC02-06CH11357. The authors thank Sungsik Lee, Benjamin Reinhart, and Jenia Karapetrova for their assistance during the experiments, and Ahmet Uysal for valuable discussions.

REFERENCES

(1) Hayes, R.; Warr, G. G.; Atkin, R. Structure and nanostructure in ionic liquids. *Chem. Rev.* **2015**, *115*, 6357−6426.

(2) Rogers, R. D.; Seddon, K. R. Ionic liquids–solvents of the future? *Science* **2003**, *302*, 792−793.

(3) Welton, T. Room-Temperature Ionic Liquids. Solvents for Synthesis and Catalysis. *Chem. Rev.* **1999**, *99*, 2071−2083.

(4) Simon, P.; Gogotsi, Y. Materials for electrochemical capacitors. *Nat. Mater.* **2008**, *7*, 845−854.

(5) Fedorov, M. V.; Kornyshev, A. A. Ionic liquids at electrified interfaces. *Chem. Rev.* **2014**, *114*, 2978−3036.

(6) Abbott, A. P.; Frisch, G.; Ryder, K. S. Electroplating Using Ionic Liquids. *Annu. Rev. Mater. Res.* **2013**, *43*, 335−358.

(7) Fedorov, M. V.; Kornyshev, A. A. Towards understanding the structure and capacitance of electrical double layer in ionic liquids. *Electrochim. Acta* **2008**, *53*, 6835−6840.

(8) Gebbie, M. A.; Valtiner, M.; Banquy, X.; Henderson, W. A.; Israelachvili, J. N. Reply to Perkin et al.: Experimental observations demonstrate that ionic liquids form both bound (Stern) and diffuse electric double layers. *Proc. Natl. Acad. Sci. U. S. A.* **2013**, *110*, E4122−E4122.

(9) Gebbie, M. A.; Valtiner, M.; Banquy, X.; Fox, E. T.; Henderson, W. A.; Israelachvili, J. N. Ionic liquids behave as dilute electrolyte solutions. *Proc. Natl. Acad. Sci. U. S. A.* **2013**, *110*, 9674−9679.

DOI: 10.1021/acscentsci.6b00014
ACS Cent. Sci. 2016, 2, 175−180

(10) Perkin, S.; Salanne, M.; Madden, P.; Lynden-Bell, R. Is a Stern and diffuse layer model appropriate to ionic liquids at surfaces? *Proc. Natl. Acad. Sci. U. S. A.* **2013**, *110*, E4121.
(11) Schmickler, W.; Santos, E. *Interfacial electrochemistry*; Springer-Verlag: Berlin, 2010; pp 1−272.
(12) Bedzyk, M. J.; Bommarito, G. M.; Caffrey, M.; Penner, T. L. Diffuse-double layer at a membrane-aqueous interface measured with x-ray standing waves. *Science* **1990**, *248*, 52−56.
(13) Kornyshev, A. A. Double-layer in ionic liquids: Paradigm change? *J. Phys. Chem. B* **2007**, *111*, 5545−5557.
(14) Kirchner, K.; Kirchner, T.; Ivaništšev, V.; Fedorov, M. V. Electrical double layer in ionic liquids: Structural transitions from multilayer to monolayer structure at the interface. *Electrochim. Acta* **2013**, *110*, 762−771.
(15) Fedorov, M. V.; Kornyshev, A. A. Ionic liquid near a charged wall: Structure and capacitance of electrical double layer. *J. Phys. Chem. B* **2008**, *112*, 11868−11872.
(16) Fedorov, M. V.; Kornyshev, A. A. Erratum: Ionic Liquid Near a Charged Wall: Structure and Capacitance of Electrical Double Layer. *J. Phys. Chem. B* **2009**, *113*, 4500.
(17) Bazant, M. Z.; Storey, B. D.; Kornyshev, A. A. Double Layer in Ionic Liquids: Overscreening versus Crowding. *Phys. Rev. Lett.* **2011**, *106*, 046102.
(18) Bazant, M.; Storey, B.; Kornyshev, A. Erratum: Double Layer in Ionic Liquids: Overscreening versus Crowding [Phys. Rev. Lett. 106, 046102 (2011)]. *Phys. Rev. Lett.* **2012**, *109*, 149903.
(19) Kilic, M. S.; Bazant, M. Z.; Ajdari, A. Steric effects in the dynamics of electrolytes at large applied voltages. I. Double-layer charging. *Phys. Rev. E* **2007**, *75*, 1−16.
(20) Ivanistsev, V.; Fedorov, M. V.; Lynden-Bell, R. M. Screening of Ion-Graphene Electrode Interactions by Ionic Liquids: The Effects of Liquid Structure. *J. Phys. Chem. C* **2014**, *118*, 5841−5847.
(21) Ivaništšev, V.; Fedorov, M. Interfaces between Charged Surfaces and Ionic Liquids: Insights from Molecular Simulations. *Electrochem. Soc. Interface* **2014**, *23*, 65−69.
(22) Kornyshev, A. A.; Qiao, R. Three-dimensional double layers. *J. Phys. Chem. C* **2014**, *118*, 18285−18290.
(23) Bowers, J.; Vergara-Gutierrez, M. C.; Webster, J. R. P. Surface Ordering of Amphiphilic Ionic Liquids. *Langmuir* **2004**, *20*, 309−312.
(24) Lauw, Y.; Horne, M. D.; Rodopoulos, T.; Lockett, V.; Akgun, B.; Hamilton, W. A.; Nelson, A. R. J. Structure of [C 4 mpyr][NTf 2] Room-Temperature Ionic Liquid at Charged Gold Interfaces. *Langmuir* **2012**, *28*, 7374−7381.
(25) Mezger, M.; Schröder, H.; Reichert, H.; Schramm, S.; Okasinski, J. S.; Schöder, S.; Honkimäki, V.; Deutsch, M.; Ocko, B. M.; Ralston, J.; Rohwerder, M.; Stratmann, M.; Dosch, H. Molecular layering of fluorinated ionic liquids at a charged sapphire (0001) surface. *Science* **2008**, *322*, 424−428.
(26) Mezger, M.; Schramm, S.; Schröder, H.; Reichert, H.; Deutsch, M.; De Souza, E. J.; Okasinski, J. S.; Ocko, B. M.; Honkimäki, V.; Dosch, H. Layering of [BMIM]+-based ionic liquids at a charged sapphire interface. *J. Chem. Phys.* **2009**, *131*, 094701.
(27) Brkljača, Z.; Klimczak, M.; Miličević, Z.; Weisser, M.; Taccardi, N.; Wasserscheid, P.; Smith, D. M.; Magerl, A.; Smith, A.-S. a. Complementary Molecular Dynamics and X-ray Reflectivity Study of an Imidazolium-Based Ionic Liquid at a Neutral Sapphire Interface. *J. Phys. Chem. Lett.* **2015**, *6*, 549−555.
(28) Zhou, H.; Rouha, M.; Feng, G.; Lee, S. S.; Docherty, H.; Fenter, P.; Cummings, P. T.; Fulvio, P. F.; Dai, S.; McDonough, J.; Presser, V.; Gogotsi, Y. Nanoscale perturbations of room temperature ionic liquid structure at charged and uncharged interfaces. *ACS Nano* **2012**, *6*, 9818−9827.
(29) Uysal, A.; Zhou, H.; Feng, G.; Lee, S. S.; Li, S.; Cummings, P. T.; Fulvio, P. F.; Dai, S.; McDonough, J. K.; Gogotsi, Y. Interfacial ionic 'liquids': connecting static and dynamic structures. *J. Phys.: Condens. Matter* **2015**, *27*, 032101.
(30) Yu, C.-J.; Richter, A.; Datta, A.; Durbin, M.; Dutta, P. Observation of molecular layering in thin liquid films using X-ray reflectivity. *Phys. Rev. Lett.* **1999**, *82*, 2326.
(31) Yamamoto, R.; Morisaki, H.; Sakata, O.; Shimotani, H.; Yuan, H.; Iwasa, Y.; Kimura, T.; Wakabayashi, Y. External electric field dependence of the structure of the electric double layer at an ionic liquid/Au interface. *Appl. Phys. Lett.* **2012**, *101*, 053122.
(32) Uysal, A.; Zhou, H.; Feng, G.; Lee, S. Structural Origins of Potential Dependent Hysteresis at the Electrified Graphene/Ionic Liquid Interface. *J. Phys. Chem. C* **2014**, *118*, 569−574.
(33) Hayes, R.; Borisenko, N.; Tam, M. K.; Howlett, P. C.; Endres, F.; Atkin, R. Double Layer Structure of Ionic Liquids at the Au(111) Electrode Interface: An Atomic Force Microscopy Investigation. *J. Phys. Chem. C* **2011**, *115*, 6855−6863.
(34) Black, J. M.; Walters, D.; Labuda, A.; Feng, G.; Hillesheim, P. C.; Dai, S.; Cummings, P. T.; Kalinin, S. V.; Proksch, R.; Balke, N. Bias-Dependent Molecular-Level Structure of Electrical Double Layer in Ionic Liquid on Graphite. *Nano Lett.* **2013**, *13*, 5954−5960.
(35) Hayyan, M.; Mjalli, F. S.; Hashim, M. A.; AlNashef, I. M.; Mei, T. X. Investigating the electrochemical windows of ionic liquids. *J. Ind. Eng. Chem.* **2013**, *19*, 106−112.
(36) Zhang, S.; Sun, N.; He, X.; Lu, X.; Zhang, X. Physical properties of ionic liquids: Database and evaluation. *J. Phys. Chem. Ref. Data* **2006**, *35*, 1475−1517.
(37) Binnig, G.; Rohrer, H.; Gerber, C.; Weibel, E. 7× 7 reconstruction on Si (111) resolved in real space. *Phys. Rev. Lett.* **1983**, *50*, 120.
(38) Sloutskin, E.; Ocko, B. M.; Tamam, L.; Kuzmenko, I.; Gog, T.; Deutsch, M. Surface Layering in Ionic Liquids: An X-ray Reflectivity Study. *J. Am. Chem. Soc.* **2005**, *127*, 7796−7804.
(39) Lockett, V.; Sedev, R.; Ralston, J.; Horne, M.; Rodopoulos, T. Differential Capacitance of the Electrical Double Layer in Imidazolium-Based Ionic Liquids: Influence of Potential, Cation Size, and Temperature. *J. Phys. Chem. C* **2008**, *112*, 7486−7495.
(40) Nishi, N.; Hashimoto, A.; Minami, E.; Sakka, T. Electrocapillarity and zero-frequency differential capacitance at the interface between mercury and ionic liquids measured using the pendant drop method. *Phys. Chem. Chem. Phys.* **2015**, *17*, 5219−5226.
(41) Schmidt, J.; Krekeler, C.; Dommert, F.; Zhao, Y.; Berger, R.; Site, L. D.; Holm, C. Ionic charge reduction and atomic partial charges from first-principles calculations of 1,3-dimethylimidazolium chloride. *J. Phys. Chem. B* **2010**, *114*, 6150−6155.
(42) Hollóczki, O.; Malberg, F.; Welton, T.; Kirchner, B. On the origin of ionicity in ionic liquids. Ion pairing versus charge transfer. *Phys. Chem. Chem. Phys.* **2014**, *16*, 16880−16890.
(43) Del Pópolo, M. G.; Lynden-Bell, R. M.; Kohanoff, J. Ab initio molecular dynamics simulation of a room temperature ionic liquid. *J. Phys. Chem. B* **2005**, *109*, 5895−5902.
(44) Youngs, T. G.; Hardacre, C. Application of static charge transfer within an ionic-liquid force field and its effect on structure and dynamics. *ChemPhysChem* **2008**, *9*, 1548−1558.
(45) Gacino, F. M.; Regueira, T.; Comunas, M. J. P.; Lugo, L.; Fernandez, J. Density and isothermal compressibility for two trialkylimidazolium-based ionic liquids at temperatures from (278 to 398) K and up to 120 MPa. *J. Chem. Thermodyn.* **2015**, *81*, 124−130.
(46) Higashi, G. S.; Chabal, Y. J.; Trucks, G. W.; Raghavachari, K. Ideal hydrogen termination of the Si (111) surface. *Appl. Phys. Lett.* **1990**, *56*, 656−658.
(47) Fenter, P.; Sturchio, N. C. Mineral−water interfacial structures revealed by synchrotron X-ray scattering. *Prog. Surf. Sci.* **2004**, *77*, 171−258.

DOI: 10.1021/acscentsci.6b00014
ACS Cent. Sci. 2016, 2, 175−180